We are IntechOpen,
the world's leading publisher of
Open Access books
Built by scientists, for scientists

4,800
Open access books available

122,000
International authors and editors

135M
Downloads

154
Countries delivered to

Our authors are among the

TOP 1%
most cited scientists

12.2%
Contributors from top 500 universities

CLARIVATE ANALYTICS

BOOK CITATION INDEX

INDEXED

WEB OF SCIENCE™

Selection of our books indexed in the Book Citation Index
in Web of Science™ Core Collection (BKCI)

Interested in publishing with us?
Contact book.department@intechopen.com

Numbers displayed above are based on latest data collected.
For more information visit www.intechopen.com

Numerical Simulation in Aortic Arch Aneurysm

Feng Gao[1], Aike Qiao[2] and Teruo Matsuzawa[3]
[1]Tokyo University of Science,
[2]Beijing University of Technology,
[3]Japan Advanced Institute of Science and Technology,
[1,3]Japan
[2]China

1. Introduction

The aorta, acting as the main conduit through which cardiac output is delivered to the systemic arterial bed, is continuously exposed to high pulsatile pressure and shear stress, making it prone to mechanical injury. It is also more prone to rupture than other vessels, particularly with the development of aneurysmal dilation. Fifty percent of patients who experience a rupture of a aortic aneurysm die before reaching the hospital (Bengtsson & Bergqvist, 1993). The incidence increases with age and has been reported as 6 per 100,000 person-years (Knowles & Kneeshaw, 2004). Aneurysmal degeneration that occurs in the aortic arch is termed a aortic arch aneurysm. Patients who have aortic arch aneurysm have multiple aortic lesions or aneurysmal disease which involves segment of aorta (Crawford et al., 1984). Aortic arch aneurysms represent only 10% of aneurysms of the thoracic aorta and it has higher risk of rupture than other aneurysm (Knowles & Kneeshaw, 2004).

Blood flow through the aorta is one of the most complex flow situations found in the cardiovascular system. Blood flow is pulsatile and pressure inside aortic aneurysm is non-uniform. The dynamics interaction between blood flow and wall may influence the wall stress. Computer modeling has made impressive progress in scientific, engineering, biological and medical applications in recent years and it offers the prospect of providing both a better insight into a range of biomechanical problems and improved tools for the design of medical devices and the diagnosis of pathologies. Computational methods such as mathematical modeling methods (Rideout, 1991; Rupnic & Runvovc, 2002; Abdolrazaghi et al., 2008), computational fluid dynamics methods, (Botnar et al., 2000; Shahcheraghi et al., 2002; Morris et al., 2005; Tokuda et al. 2008) loosely coupled methods (Di Mrrtino et al., 2001; Gao et al., 2006abc) have been used to simulate the biomechanical problems in arotic arch and aortic arch aneurysm. The aim of this chapter is to describe the numerical simulation and computer modeling work in aortic arch aneurysm.

2. Aorta, aortic arch and structure of aortic wall

Arteries are vessels that carry blood away from the heart. The aorta is the largest artery in the body (Fig. 1). It arises from the left ventricle of the heart, forms an arch, and then extends down to the abdomen where it branches off into two smaller arteries. It consists of the

ascending aorta, the aortic arch, and the descending aorta. Ascending aorta extends upward from the aortic root to the point where the innominate artery branches off the aorta, and the aorta begins to form an arch. Aortic arch represents the curved portion at the top of the aorta. Descending aorta begins just beyond the arch as the aorta bends down into the body. It carries and distributes oxygen rich blood to all arteries.
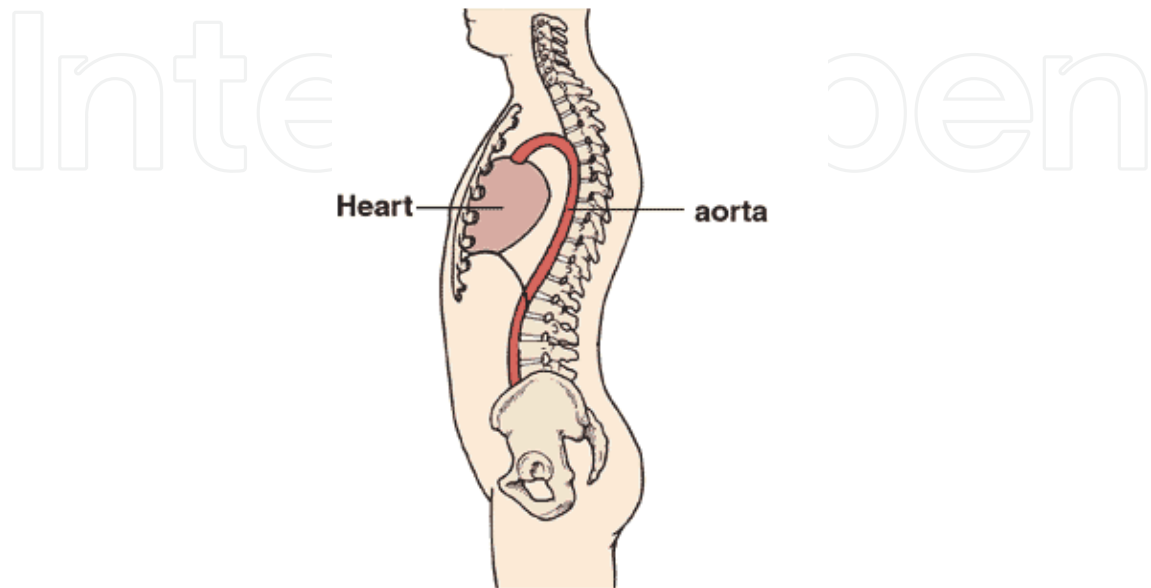

Fig. 1. Aorta in the human body. It arises from the left ventricle of the heart, forms an arch, and then extends down to the abdomen.

The aorta is distinguished by their great elasticity. This helps them smooth out the large fluctuations in blood pressure created by the heartbeat. In order to understand the properties of aorta, the three types of arteries should first be mentioned. These are elastic arteries, medium muscular arteries, small arteries and arterioles. For aorta, large arteries and small arteries, the typical radius, typical length, and typical numbers are shown in Table 1.

Vessel	Typical radius (mm)	Typical length (mm)	Typical number
Aorta	12	500	1
Large arteries	3	250	50
Small arteries	1	50	2×10^3

Table 1. The typical radius, length, and numbers for aorta, large arteries and small arteries.

Elastic arteries experience the greatest pressures and are closest to the heart. The aorta is the largest elastic artery that delivers blood from the left ventricle of the heart to the rest of the body. Aorta is described as arteries that contain more elastin than smooth muscle content in the media. The elastin is necessary to allow the vessel to expand and recoil during pulsatile flow (Benjamin Cummings, 1996). The current investigation will work with the elastic artery, such as the aorta (throracic and abdominal) and carotid arteries (Yamada, 1970). The innermost layer is the tunica intima. The middle layer is the tunica media and the outermost layer is the tunica adventitia.

In general, the overall mechanical properties of the arterial wall are determined by how different compositions of collagen, elastin and protein are linked. The general rule is that when the elastin ratio is higher than the collagen ratio, the elastic modulus decreases and distensibility increases and vice versa (Doublin & Rovick, 1969). The Young's modulus of three layers of the aorta wall is different. Xie et al. (1995) did the bending experiments of blood vessel wall and found that the Young's modulus of the inner layer (intima and media) was three to four times larger than that of the outer layer (adventitia). The elastic modulus of arterial wall became a little higher after de-endothelization in Fischer's experiments (Fischer et al., 2002) and this means the elasticity of intima is lower than the mean elasticity of vessel wall since the intima layer mainly consists of endothelial cells.

3. Computational geometric reconstruction of aortic arch aneurysm

The geometric modeling is the fundamental part of the aorta modeling analysis. Owing to the complex geometry of the aorta, three-dimensional models of aorta and aortic aneurysm are considerably important. Advances in imaging are being introduced initially as research tools and subsequently as clinical diagnostic tests. The reconstruction of aorta structures involves the use of sets of clinical data (MRI or CT) that are processed to extract the vessel morphology.

3.1 STL format of aortic arch aneurysm model

Stereo lithography (STL) describes a raw unstructured triangulated surface by unit normal and vertices (ordered by the right-hand rule) of the triangles using a threedimensional Cartesian coordinate system. The surface is logically tessellated or broken down into a series of small triangles (facets). Each facet is described by a perpendicular direction and three points representing the vertices (corners) of the triangle. Point cloud and connectivity matrix data written in this format can be imported into a variety of CAD or grid generation software. A patient-specific aortic arch aneurysm model in STL format was reconstructed from CT medical images (Fig. 3). This model is a surface model in geometry, which cannot be used for numerical simulation directly (Fu et al., 2008). Reverse engineering software Geomagic and Pro/E were used to process the surface model of STL format to rebuild a patient-specific model of aortic arch aneurysm that can be used in numerical simulation.
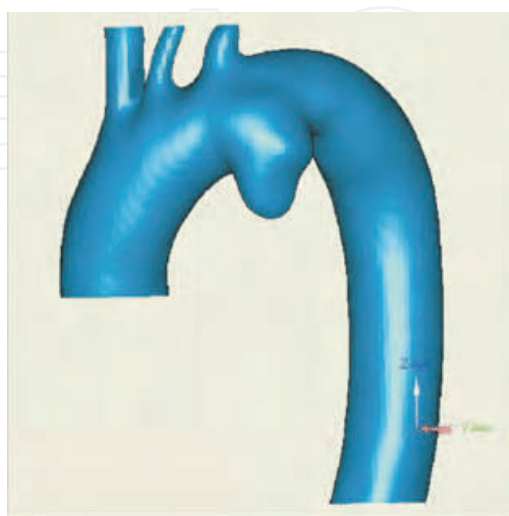

Fig. 3. A patient-specific aortic arch aneurysm model of STL format

3.2 Method of aortic arch aneurysm model reconstruction
3.2.1 Processing STL surface model

Because the boundaries of the three branches will impact the integration of patch arrangement and lead to the failure of creating NURBS (Non-Uniform Rational B-Splines) surface, the main purpose of this study is also to find a way to construct the aneurysm model, it is necessary to simplify the three branches.

1.   Simplifying surface

Opening the STL formatted surface model of the aortic arch aneurysm in Geomagic. First, cut the three branches using the "section by plane" mode. Then erase red boundaries (the boundary line after intersecting) of the incisions using the "sandpaper" and "relax" function, thus the simplified surface model is composed of closed areas with only two closed boundaries at the ends.

2.   Dividing areas

To regularly arrange patches, the method of "section by plane" was applied to divide the model into several orbicular areas. There are some rules to obey when locating the cutting plane: to preserve the changing information of geometry as much as possible; to divide more annulus at the place where shapes change sharply; approximately keeping the normal vector of the cutting plane and the trend of vessel's growth in the same direction.

3.   Rectifying arrangement of the patches

Create triangle patches under the curvature level 0.3 by using "detect curvature" in "detect curvature" mode. Delete extra orange boundaries (panel-demarcation line) and rectify arrangement of the patches manually to make sure each red boundary with only four keypoints. The arrangement of each opposite keypoints must vary with the changed area to avoid torsion around the direction of the bloodstream.

4.   Checking and output

After checking and repairing the arrangement of quadrilateral patches with "repair patches" function, NURBS surface fitted with 48 pieces of quadrilateral patches was finally created. Then export this NURBS surface model in IGES format.

3.2.2 Reconstructing solid model

1.   Preprocessing areas

Open the NURBS surface model in Pro/E. Create planes that are parallel to the former red closed boundaries and get intersection lines. Each intersection line is composed of four lines connected end to end.

2.   Creating solid part

Based on the former intersection lines, a solid model was created by blended drawing.

3.   Reconstructing three branches

Because the shape near the three branches is very complicated and irregular, precise measurement is difficult in CAD software. Considering some small differences are not important and have little influence on the following works, therefore, it is viable to make some hypotheses and simplifications for convenient rebuilding of branches. Branches and aortic arch were connected with round chamfer; cross sections were simplified as circle or ellipse; and the centers were located through eyeballing. Based on these simplifications, three branches were reconstructed using software Pro/E.

4.   Creating boundary layer

The thickness of the boundary layer is related with the velocity, factor of friction, location, shape, etc. Even at the same place, the thickness of the boundary layer may be different at

different times. To gradually obtain finer grids in the boundary layer in the following meshing procedure, a solid shell was primarily constructed to approximately imitate the boundary layer. Because the thickness of the boundary layer is extremely thin and uncertain, an assumed layer thickness not less than 10% of the maximal diameter is sufficient for the boundary layer and easy to construct. Create circle and ellipse lines in the former planes that are parallel to the former red closed boundaries. Place centers near the centroid. Choose inner diameter not more than 80% of the maximal distance of the section. To avoid the situation where stents cross the boundary layer, properly move some centers away from the aneurysm and reduce the inner diameter to about 20%–60% of the maximal distance of the section. A shell remained after cutting a hollow by blended drawing (Fig. 4).
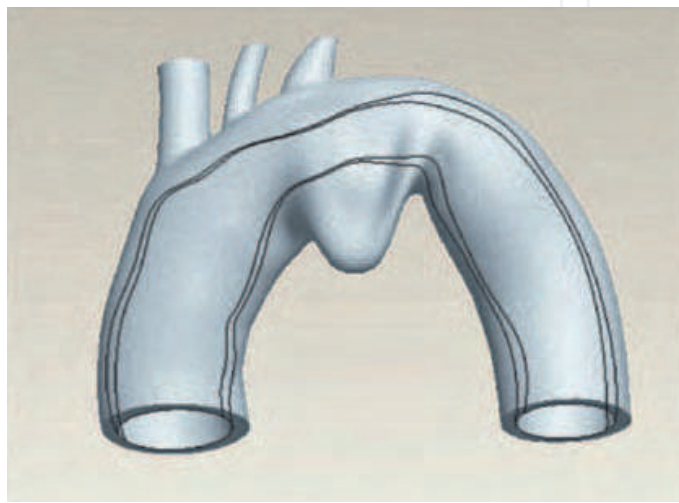

Fig. 4. Reconstructed solid model of aortic arch aneurysm for numerical simulation

4. Simulation in aortic arch and aortic arch aneurysm

4.1 Mathematical modeling on aortic aneurysm

It was Stephen Hales in his Statistical Essays who considered arterial elasticity and postulated its buffering effect on the pulsatile nature of blood flow (Hales, 1733). He likened the depulsing effect to the fire engines of his day, in which a chamber with an air-filled dome acted to cushion the bolus from the inlet water pump so that "a more nearly equal spout" flowed out the nozzle. This analogy became the basis of the first modern cardiovascular models. In the translation from English to German, Hales' s inverted globe became a windkessel (air kettle); his idea later became known as the Windkessel theory when it was more formally developed and propounded by the German physiologist Otto Frank near the beginning of our century (Noordergraaf, 1978).

A short segment of aorta can be modeled by an elastic, isobaric chamber attached to a rigid inlet and outlet tube. The ability of the chamber to store fluid depends on its compliance, C, which is defined as

$$C = \frac{dV_c}{dP_c} \tag{1}$$

where V_c is total segment (chamber) volume and P_c is chamber pressure. Many modelers prefer to use the reciprocal of compliance (termed stiffness, S, or elastance, E). Here,

viscoelastic (stress relaxation) effects are assumed negligible, so that compliance is not an explicit function of time. Thus, compliance becomes an instantaneous variable which can be obtained from the experimentally determined, steadystate pressure-volume (*P-V*) relationship of the segment. Furthermore, model order can be reduced, as pressure can be mathematically represented as an empirical function of volume, either by a piecewise linear approximation, a polynomial quotient, or some other function fit to the *P-V* relationship. A typical *P-V* curve is illustrated in Fig. 5, along with its piecewise liner approximation. In arteries, pressure is usually positive with small oscillations about a nominal operating point (point a in Fig. 5). Hence the piecewise linear approximation can be reduced to a single line with constant slope $1/C$:

$$P_c = \frac{\left(V_c - V_{c_0}\right)}{c} \tag{2}$$

where V_{c0} is the unstressed volume (the idealized zero-pressure volume intercept). Of course, if pressure fluctuates outside this region, then additional straight-line sections should be included.
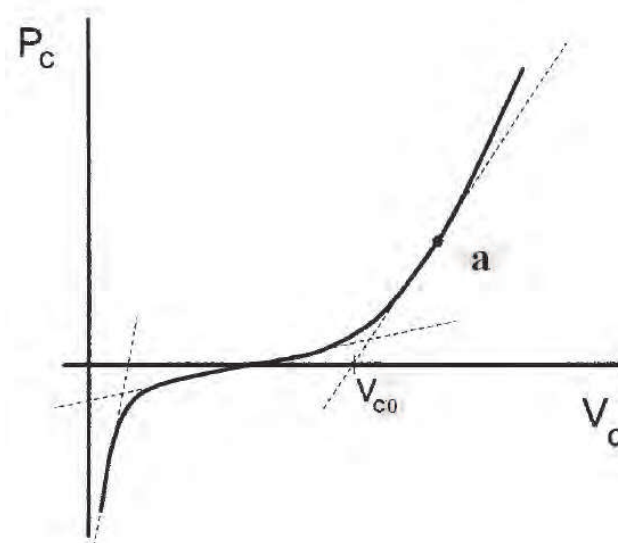

Fig. 5. Pressure-volume relationship of aorta

Assuming that blood is incompressible and newtonian, that the flow profile is parabolic and unchanging with axial distance along a straight rigid tube, then flow (poisenillean) is linearly proportional to the pressure gradient across the ends of the tube. Hence, flow into and out of the chamber may be calculated given P_{in} and P_{out} (the inlet and outlet pressures); P_c; L_{in} and L_{out} (the inertances due to fluid mass); and R_{in} and R_{out} (the resistances due to viscous drag)

$$L_{in} \frac{df_{in}}{dt} + R_{in} f_{in} = P_{in} - P_c \tag{3}$$

$$L_{out} \frac{df_{out}}{dt} + R_{out} f_{out} = P_c - P_{out} \tag{4}$$

where f_{in} and f_{out} are the flows into and out of the segment. Volume can now be calculated from the difference between the inlet and outlet flows: P_c, V_c, f_{in}, and f_{out} can now be uniquely determined at any time given P_{in}, P_{out}, and the initial conditions of the segment. Determination of the parameters L and R are more problematic. They can be derived analytically, although probably because the modeling assumptions are not completely correct, an empirical fit generally produces better segmental properties.

$$\frac{dV_c}{dt} = f_{in} - f_{out} \tag{5}$$

The mathematical modeling method has been applied to the cardiovascular system for the study of system pathologies (Rideout, 1991; Rupnic & Runvovc, 2002). The aortic aneurysm has primarily been probed and the compliance of aortic aneurysms was investigated and the effects of the pathology were observed (Long et al., 2004; Morris-Stiff et al., 2005). The cardiac pressure-volume loops for aortic aneurysms has been presented by utilizing electronic cardiovascular modeling (Abdolrazaghi et al., 2008). The electronic parameters are correlated to their mechanical parameters as follows: voltage is analogous to pressure, capacitance to compliance, and inductance to inertance. The aortic aneurysm with different diameters were applied and left ventricle pressure-volume with aortic aneurysm increased. There is significant increase in pressure both in thoracic and abdominal aortic aneurismal condition, therefore it can be understood that the hypertension could be principal symptom of these disease (Abdolrazaghi et al., 2008).

4.2 Hemodynamics simulation in aortic arch and aortic aneurysm

Blood flow through the aorta is one of the most complex flow situations found in the cardiovascular system. This is mainly due to the strong curvature effects, irregular geometry, tapering and branching. The human aortic arch has a characteristic configuration. One of its characteristics is that the centerline of the arch does not lie in a plane. Another is that there are major branches at the top of the arch. Kilner et al. (1993) observed a characteristic helical blood flow pattern in the human aortic arch using magnetic resonance measurements, and showed the qualitative flow structure in the arch. However, it is difficult to obtain distribution and transient change in the wall shear stress from measuring clinical images. Instead of experimental methods, the detailed flow in human arteries can be studied by using computational fluid dynamics methods (Botnar et al., 2000). The highly disturbed flow patterns that have been reported in regions of arterial branching and curvature are attributable to a large degree to the combined effects of complex arterial geometry and flow pulsatility. One vascular site within which the fluid mechanical environment is especially complex is the region of the aortic arch and its major branches. The arch is characterized by extensive curvature, which would be expected to lead to velocity profile skewness as well as to complex secondary flow motion. Furthermore, the three aortic arch branches which emerge in different planes are likely to have a large impact on the flow field.

A few computational studies have been made of steady and unsteady blood flow in the human aortic arch (Shahcheraghi et al., 2002; Morris et al., 2005; Tokuda et al., 2008). The simulation results demonstrate that the primary flow velocity is skewed towards the inner aortic wall in the ascending aorta, but this skewness shifts to the outer wall in the descending thoracic aorta. Within the arch branches, the flow velocities were skewed to the distal walls with flow reversal along the proximal walls. Extensive secondary flow motion

was observed in the aorta, and the structure of these secondary flows was influenced considerably by the presence of the branches. Within the aorta, wall shear stresses were highly dynamic, but were generally high along the outer wall in the vicinity of the branches and low along the inner wall, particularly in the descending thoracic aorta. Within the branches, the shear stresses were considerably higher along the distal walls than along the proximal walls. Wall pressure was low along the inner aortic wall and high around the branches and along the outer wall in the ascending thoracic aorta.
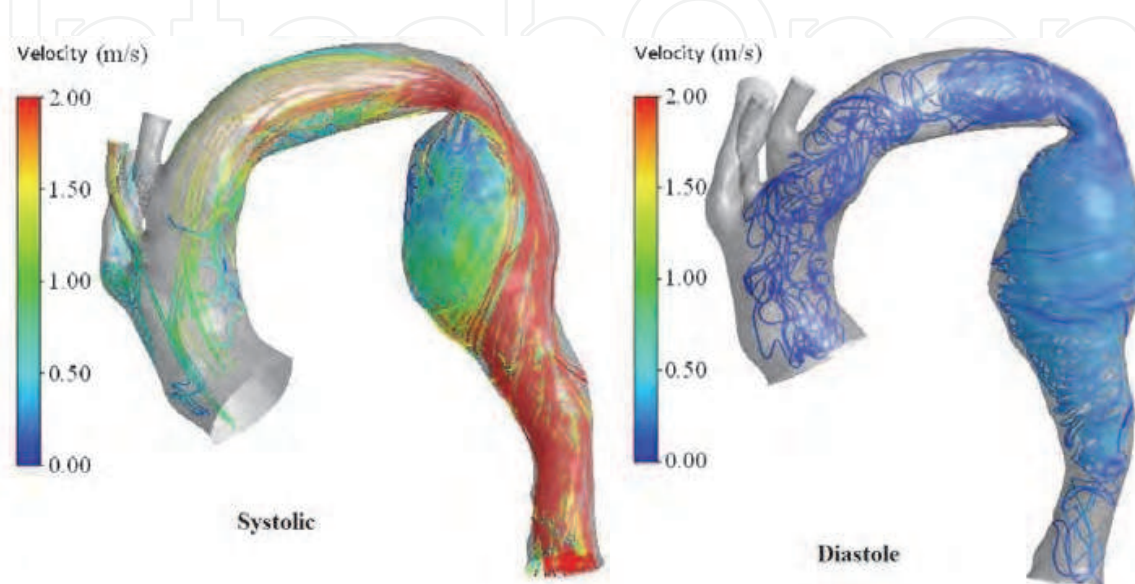

Fig. 6. Streamline of blood flow at systolic and diastole in aortic arch aneurysm

For more realistic simulation of patient-specific thoracic aneurysm blood flow, a real vasclar model containing ascending aorta, aortic arch and descending thoracic aorta was constructed basd on CT images (Qiao et al., 2011). This model also contains the innominat artery, left common carotid artery and left subclavian artery. More importantly, there is a fusiform aneurysm in the descending thoracic aorta. In arch aneurysm model, the velocity vectors illustrate a streamline profile with vortices through the aneurysm. Streamlines in an aortic arch aneurysm model at the decreasing phase of systolic and the phase of diastole are shown in Fig. 6. There was large vortexes in the descending aortic aneurysm cavity. This was the main difference of flow characteristics in the thoracic aorta with aneurysm and without aneurysm. In diastolic flow vortex characteristics were more apparent, and there were several vortices; especially in the latter half of the diastolic phase, there was a large vortex of blood flow in the descending aortic aneurysm. Therefore residence time of blood cells and other particles in the cavity of the aneurysm was increased, and the probability that these particles were deposited on these positions increased too. Those factors would increase the growth of aneurysm.

4.3 Fluid structure interaction simulation in layered aortic arch and aortic aneurysm
Although the exactly relationship between the elastic properties of intima layer and that of media layer hasn't been decided, we can deduce from the Fischer's experiment data (Fischer et al., 2002)that the Young's modulus of intima layer is smaller than that of media layer. In this present study, the Young's modulus of intima layer is assumed three times larger than that of media layer, as same as the adventitia layer:

$$3E_i = E_m = 3E_a \tag{6}$$

where E_i, E_m and E_a are the Young's modulus of intima layer, media layer and adventitia layer, respectively. The mean Young's modulus of vessel wall is same, based on the assumption that the Young's modulus of layer is in inverse proportion to the volume of layer, so:

$$E_i \cdot V_i + E_m \cdot V_m + E_a \cdot V_a = E \cdot V \tag{7}$$

where V_i, V_m, V_a and V are the volume of intima layer, media layer and adventita layer, respectively. Using the volume equation, Equation 6 becomes:

$$E_i \cdot t_i + E_m \cdot t_m + E_a \cdot t_a = E \cdot t \tag{8}$$

where t_i, t_m, t_a and t are the thickness of intima layer and that of medial layer, respectively.
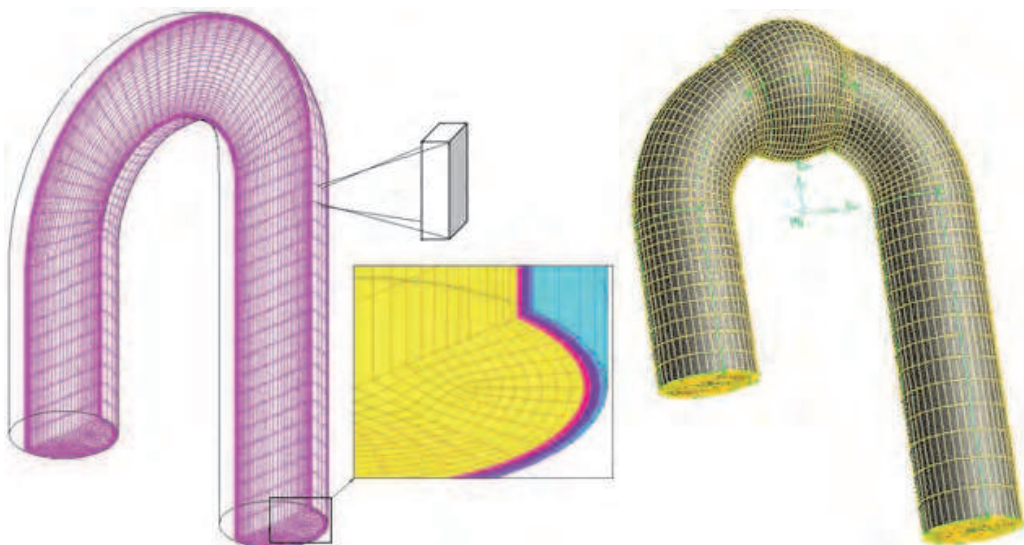

Fig. 7. Three-layered aortic arch model and aneurysm model

In cardiovascular biomechanics one of the major topics today is the simulation and analysis of the fluid-structure interaction of the cardiovascular system using computational methods (Taylor, 1999). Di Martino and colleagues (Di Mrrtino et al., 2001) provided the notion of interaction between solid and fluid domains as it contributes to aneurysm rupture potential. Fluid-structure interaction (FSI) of the domains allows computation of the flow and pressure fields in the aneurysm, simultaneously with the wall stresses.

We performed the fluid structure interaction simulation in three-layered aortic arch model (Gao et al., 2006abc). Fig. 7 shows the three-layered aortic arch model and aneurysm model. The velocity in the entrance region of the ascending aorta is blunted and skewed towards the inner wall of the aortic arch and the values become higher at the side of inner wall. Skewing is more marked in mid ascending portion. Downstream of the top arch, however, skewing of the velocity reverses, and the location of maximum velocity shifted towards the outer wall of aortic arch, which agrees with previous studies (Shahcheraghi et al., 2002).

The variations of stresses along the arch were not uniform, due to the arch structure. The circumferential stress gets first peak at the mid ascending portion and second peak at the mid descending portion and it would be unpredictable by using Laplace's Law. Hence, the shape of the arch and the hemodynamic forces acting on the vessel wall (Liepsch, 2002) may play important roles in aorta mechanics. The longitudinal stress gets its peak values at the entrance to the ascending portion and the top of the arch and the distal end of the arch.
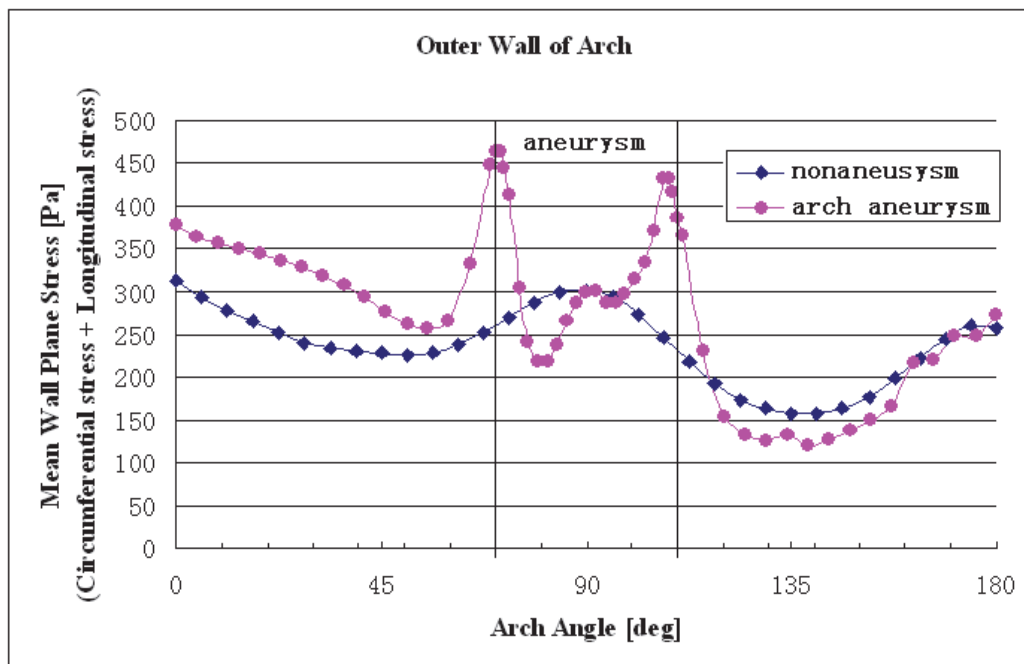

Fig. 8. Comparisons of wall stress distribution in nonaneurysm model and aneurysm model for compose stress (circumferential stress+longitudinal stress).

The FSI simulation was also performed on aortic arch aneurysm model (Gao et al., 2008). Fig. 8 shows composite stress (composition of the circumferential stress vector and the longitudinal stress vector) in aneurysm model comparing with nonaneurysm model. The wall stresses on aneurysm model were indicated to be complexly distributed with large regional variations at inflection points. The wall stresses on nonaneurysm model was relatively low and uniformly distributed. The previous study found that the failure strength of aneurysm wall was lower than that of nonaneurysm wall (Vorp et al., 1996) and the peak wall stress on aneurysm was from 45% to 69% of its failure strength, whereas the peak wall stress of nonaneurysm aorta was less than 10% of its failure strength (Raghavan et al., 2000). The maximum stresses occur at the proximal and distal ends of aneurysm. This result suggests that maximum stresses do not occur at the location of the maximum diameter but at the regions of high curvature that are associated with the proximal and distal ends. It agrees with previous studies (Raghavan et al., 2000; Di Martino et al., 2001; Vorp et al., 1998). Most aneurismal ruptures occur at the posterolateral wall, which correlates to the areas of high stress concentrations (Raghavan et al., 2000; Vorp et al., 1998). Also the actual propensity for rupture for another surface of aneurysm depends on the comparative local value of wall strength, since it was found that the strength of tissue near the neck or undilated ends of aneurysm are greater than that in the midsection, where diameter is maximum.

The arterial stiffness was significantly higher in aneurysm wall compared with healthy aortic wall (Di Martino et al., 2001; Sonesson et al., 1997). It has been suggested that aneurysms develop as a result of an alteration in the connective tissue metabolism and this might change arterial wall stiffness (Sonesson et al., 1997). Our results indicated that wall stiffness in aneurysms increase maximum stresses in inflection points. So wall stiffness in aneurysm might make the stress more increased in aneurysm. Morris et al. (2005) used the photoelastic method to simulate the failures at the proximal end and distal end of aneurysm model. It was also reported that aortic dissection originated in a distal aortic arch aneurysm (Tsukamoto et al., 2003). Arterial stiffness that increased both with age and certain disease may increase cardiovascular risk (Blacher et al., 1999). The main structural alterations at the site of the large artery media account for arterial stiffening (Benetos, 2003). The aortic wall has multi-layered composite structure and stress can not be assumed uniformly distributed through the wall thickness. The non-homogeneous stress distribution through wall thickness was showed (Fig. 9) and stresses are found to be higher in the media and reach a peak value in the media near the adventitia at inflection points and the medial stiffening increased the stress in media and peak value.
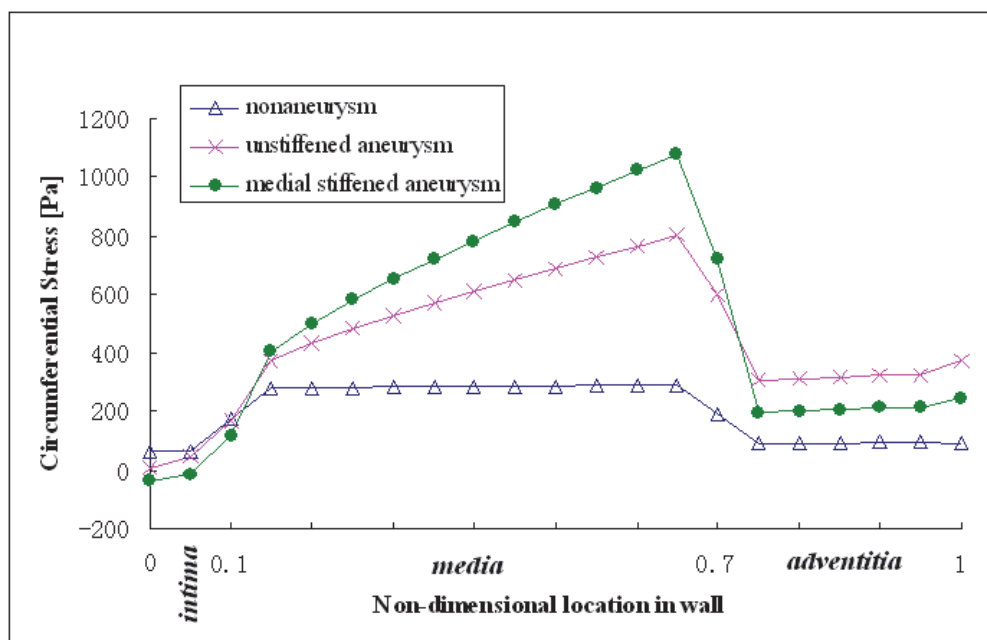

Fig. 9. Comparisons of wall stress distribution across wall for nona neurysm wall, unstiffened aneurysm wall, stiffened aneurysm wall.

4.4 Simulation in stented aortic arch aneurysm

The traditional treatment requires open surgical repair, which involves an incision and exclusion of the diseased aneurysm with a synthetic graft. An alternative treatment is endovascular aneurysm repair. Endovascular stent is commonly used to bridge the aneurysmal orifice since the first trial of Parodi (Parodi et al., 1995). Endovascular aneurysm repair is a minimally invasive technique to treat aneurysms. An endovascular graft is guided from the iliac to the affected aortic segment to shield the aneurysm from blood pressure, eliminate blood circulation in the aneurysm intrasac, and hence prevent aneurysm rupture.

Different numerical studies have focused on the hemodynamic changes in aneurysm with and without a stent-graft. Despite of the expansive investigation in the endovascular stent for aneurysms, studies of hemodynamics simulation of stented aneurysm at the aortic arch with a localized outpouching (bleb) on top of the dome, at which point aneurysms frequently rupture, are relatively rare. The hemodynamics in fully stented aortic arch aneurysms harboring a bleb has been studied on the dome (Fig. 10) (Qiao et al., 2005). The flow near the dome of the aneurysm is more sluggish after stenting, and flow activities deep within the blebs of the stented aneurysm models are significantly diminished, which agree very well with the studies of Aenis et al. (1997), Lieber et al. (2002) and Liou and Liou (2004). Stenting reduces the momentum transfer from the parent vessel to the aneurysm, thus reducing intra-aneurysmal flow, which produces thrombosis formation and subsequent contraction of the dilated aorta. The simulation results showed that the intra-aneurysmal flow in the stented aneurysm was significantly attenuated, and the pressure and WSSs were decreased. A high pressure zone at the dome of the aneurysm prior to stenting decreases after stent implantation, this phenomenon in the simulation also accords with the results of Aenis et al. (1997) and Liou and Liou (2004). The magnitude and pulsatility of the WSSs along the aneurysmal wall were reduced by stenting, specifically in the bleb region. Considering the widely convinced therapeutic mechanism of endovascular stents, we believe that the stent-induced sluggish flow activity, low pressure, low WSS and hence embolization in the aortic arch aneurysmal sacs can facilitate the occlusion of aneurysms. The hemodynamic characteristics allow us to conclude that we can treat aortic arch aneurysm with bare wire-mesh endovasucular stents.
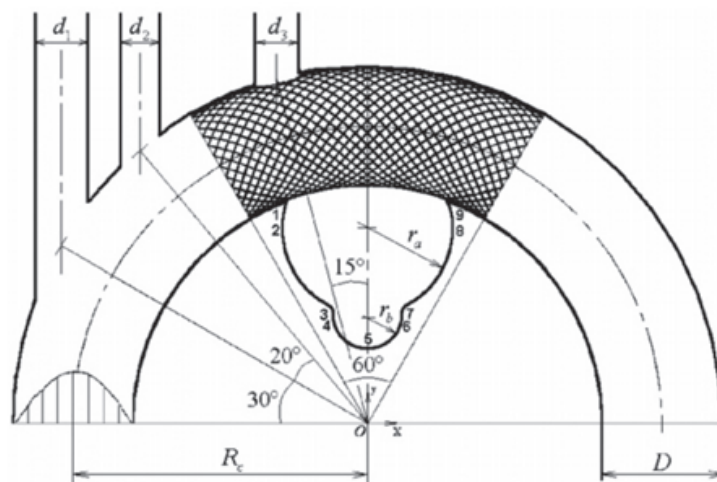

Fig. 10. Geometric models of the stented aortic arch aneurysm harboring a bleb on its dome.

The shape of the stent (e.g., helix-versus mesh-shaped stents) (Liou et al., 2004), the size of the orifice, the porosity of a stent (Rhee et al., 2002) and the stent filament size (Lieber et al., 2002; Bando & Berger, 2003) are important factors that influence the treatment effectiveness of stented aneurysms. The hemodynamics simulations concerning the optimization of all these factors are still open to question. Other prospective approaches, such as stent-graft (Chuter et al., 2003) (covered stent, coated by porous polyurethane) (Ruiz et al., 1995), coiling (Asakura et al., 2003), and multiple overlapping stents (Doerfler et al., 2004), are emerging as therapeutic alternatives to surgery for the treatment of aneurysms, and are under way for clinical trial.

5. Conclusion

The aorta is continuously exposed to high pulsatile pressure and shear stress, making it prone to mechanical injury. Aneurysmal degeneration that occurs in the aortic arch is termed a aortic arch aneurysm. It has higher risk of rupture than other aneurysm.

The computational modeling in aortic arch aneurysm was designed, implemented and evaluated using a series of technologies-based tools. These tools modeled the biomechanical aspects of aortic arch aneurysm. The computational modeling presented in the chapter combined imaging data, geometrical reconstruction, hemodynamics, the interaction between blood flow and aortic wall, and the effect of endovascular stent. The developed modeling will aid research and ensure that medical professionals benefit through the precise information about aortic arch aneurysm. It will also improve the accuracy and efficiency of the medical procedures.

6. References

Abdolrazaghi, M.; NavidBakhsh, M. & Hassani, K. (2008). Abdominal and Thoracic Aortic Aneurysm Modeling. *American Journal of Applied Science* Vol.5(8), pp. 1052-1058.

Aenis, M.; Stancampiano, A.P.; Wakhloo, A.K. & Lieber, B.B. (1997). Modeling of flow in a straight stented and nonstented side wall aneurysm model. *J. Biomech. Eng.* Vol.119, pp.206–212.

Asakura, F.; Tenjin, H.; Sugawa, N.; Kimura, S. & Oki, F. (2003). Evaluation of intra-aneurysmal blood flow by digital subtraction angiography: Blood flow change after coil embolization. *Surg. Neurol.* Vol.59, pp.309–318.

Bando, K. & Berger, S.A. (2003). Research on fluid-dynamic design criterion of stent used for treatment of aneurysms by means of computational simulation. *Comput. Fluid Dyn. J.* Vol.11, pp.527–531.

Benetos, A. (2003). Pulse pressure and arterial stiffness in type 1 diabetic patients. *Journal of Hypertension,* Vol.21, pp.2005-2007.

Bengtsson, H.; Bergqvist, D. (1993). Ruptured abdominal aortic aneurysm: a population-based study. *J Vasc Surg* Vol.18, pp. 74–80.

Blacher, J.; London, G.M. & Safar, M.E. (1999). Influence of age and end-stage renal disease on the stiffness of carotid wall material in hypertension. *J. Hypertens.*, Vol.17, pp.237-244.

Botnar, R.; Rappitsch, G.; Scheidegger, M.B.; Liepsch, D.; Perktold, K. & Boesiger, P. (2000). Hemodynamics in the carotid artery bifurcation: a comparison between numerical simulations and in vitro MRI measurements. *J Biomech.* Vol.33(2), pp.137-44.

Chuter, T.A.M.; Schneider, D.B.; Reilly, L.M.; Lobo, E.P. & Messina, L.M. (2003). Modular branched stent graft for endovascular repair of aortic arch aneurysm and dissection. *J. Vasc. Surg.* Vol.7, 859–863.

Crawford, E.S.; Stowe, C.L.; Crawford, J.L.;Titus, J.L. & Weilbaecher, D.G. (1984). Aortic arch aneurysm. A sentinel of extensive aortic disease requiring subtotal and total aortic replacement. *Ann Surg.* Vol.199(6), pp. 742-52.

Di Martino, E.S.; Guadagni, G.; Fumero, A.; Ballerini, G.; Spirito, R.; Biglioli, P. & Redaelli, A. (2001). Fluid-structure interaction within realistic threedimensional models of

the aneurysmatic aorta as a guidance to assess the risk of rupture of the aneurysm. *Medical Engineering and Physics* Vol.23, pp.647-655.

Di Martino, E.S.; Guadagni, G.; Fumero, A.; Ballerini, G.; Spirito, R.; Biglioli, P.; Redaelli, A. (2001). Fluid-structure interaction within realistic three-dimensional models of the aneurysmatic aorta as a guidance to assess the risk of rupture of the aneurysm. *Med. Eng. Phys.*, Vol. 23, pp.647-655.

Doerfler, A.; Wanke, I.; Egelhof, T.; Stolke, D. & Forsting, M. (2004). Double-stent method: therapeutic alternative for small wide-necked aneurysms. Technical note. *J. Neurosurg.* Vol.100, pp.150–154.

Doublin, D.B. & Rovick, A.A. (1969). Influence of vascular smooth muscle on contractile mechanics and elasticity of arteries. *Americal Journal of Physiology,* Vol. 217, pp.1644-1651.

Fischer, E.I.; Armentano, R.L.; Pessana, F.M.; Graf, S.; Romero, L.; Christen, A.I.; Simon, A. & Levenson, J. (2002). Endothelium-dependent arterial wall tone elasticity modulated by blood viscosity, Am. J. Physiol. Heart Circ. Physiol. Vol.282, pp.389-394.

Fu, W. Y.; Qiao, A.K. & Fu, P. (2008) Boundary identification and triangulation of STL model. In: *Proceeding of the first International Conference on Biomedical Engineering and Informatics.* Sanya, pp. 27–30

Gao, F.; Guo, Z.; Sakamoto, M. & Matsuzawa, T. (2006a). Fluid-structure Interaction within a Layered Aortic Arch Model. *Journal of Biological Physics,* Vol.32, pp.435-454.

Gao, F.; Guo, Z.; Watanabe, M. & Matsuzawa, T. (2006b). Loosely Coupled Simulation for Aortic Arch Model under Steady and Pulsatile Flow, *Journal of Biomechanical Science and Engineering,* Vol.1, pp.327-341.

Gao, F.; Watanabe, M. & Matsuzawa, T. (2006c). Stress analysis in a layered aortic arch model under pulsatile blood flow. *BioMedical Engineering OnLine,* Vol.5:25.

Gao, F.; Ohta O. & Matsuzawa, T. (2008). Fluid-structure interaction in layered aortic arch aneurysm model: Assessing the combined influence of arch aneurysm and wall stiffness. *Australas. Phys Eng Sci Med.* Vol. 31, pp.32-41.

Kilner, P.J.; Yang, G.Z.; Mohiaddin, R.H.; Firmin, D.N. & Longmore, D.B. (1993). Helical and retrograde secondary flow patterns in the aortic arch studied by three-directional magnetic resonance velocity mapping. *Circulation.* Vol.88(5 Pt 1), pp.2235-2247.

Knowles, A.C. & Kneeshaw, J.D. (2004). Aortic arch surgery. In: Mackay JH, Arrowsmith JE (Eds). *Core Topics in Cardiac Anaesthesia.* London: Greenwich Medical Media. pp.191-194.

Lieber, B.B.; Livescu, V.; Hopkins, L.N. & Wakhloo, A.K. (2002). Particle image velocimetry assessment of stent design influence on intraaneurysmal flow. *Ann. Biomed. Eng.* Vol.30, pp.768–777.

Liou, T.M. & Liou, S.N. (2004). Pulsatile flows in a lateral aneurysm anchored on a stented and curved parent vessel. *Exp. Mech.* Vol.44, pp.253–260.

Liou, T.M.; Liou, S.N. & Chu, K.L. (2004). Intra-aneurysmal flow with helix and mesh stent placement across side-wall aneurysm pore of a straight parent vessel. *J. Biomech. Eng.* Vol.126, pp.36–43.

Long, A.; Rouet, L. & Bissery, A. (2004). Compliance of abdominal aortic aneurysms: Evaluation of tissue Doppler imaging. *J. Ultrasound in Medical and Biology,* Vol.30, Vol.1099- 1108.

Morris, L.; Delassus, P.; Callanan, A.; Walsh, M.; Wallis., F.; Grace, P & McGloughlin, T. (2005). 3-D numerical simulation of blood flow through models of the human aorta. *J Biomech Eng* Vol.127(5), pp.767−75.

Morris-Stiff, G.; Haynes, M. & Ogunbiyi, S. (2005). Is Assessment of Popliteal Artery Diameter in Patients Undergoing Screening for Abdominal Aortic Aneurysms a Worthwhile Procedure. *European Journal of Vascular and Endovascular Surgery,* Vol.30, pp. 71-74.

Qiao, A.K.; Fu, W.Y. & Liu, Y.J. (2011) Study on hemodynamics in patient-specific thoracic aortic aneurysm, *Theor. Appl. Mech. Lett.* Vol. 1 (1), 014001-1-4

Raghavan, M.L.; Vorp, D.A.; Federle, M.P.; Makaroun, M.S. & M.W. Webster, M.W. (2000) Wall stress distribution on three-dimensionally reconstructed models of human abdominal aortic aneurysm. *J. Vasc. Surg.,* Vol.31, pp.760-769.

Rideout, V.C. (1991). Mathematical and computer modeling of physiological systems. New York: Prentice Hall.

Rupnic, M. & Runvovc, F. (2002). Simulation of steady state and transient phenomena by using the equivalent electronic circuit. *J. Computer Methods and Programs in Biomedici.,* Vol. 67, pp.1-12.

Shahcheraghi, N.; Dwyer, H.A.; Cheer, A.Y.; Barakat, A.I. & Rutaganira, T. (2002). Unsteady and three-dimensional simulation of blood flow in the human aortic arch. *J Biomech Eng* Vol.124(4), pp.378-387.

Sonesson, B.; Hansen, F. & Lanne, T. (1997). Abdominal aortic aneurysm: a general defect in the vasculature with focal manifestations in the abdominal aorta?. *J. Vasc. Surg.,* Vol. 26(2), pp.247-254.

Taylor, C.A. (1999). Predictive medicine: computational techniques in therapeutic decision-making. *Computer Aided Surgery,* 4:231-247, 1999.

Tokuda, Y; Song, M.H.; Ueda, Y.; Usui, A.; Akita, T.; Yoneyama, S. & Maruyama, S. (2008). Eur J , Three-dimensional numerical simulation of blood flow in the aortic arch during cardiopulmonary bypass. *Cardiothorac Surg.* Vol. 33(2), pp.164-7

Tsukamoto, S.; Shindo, S.; Obana, M.; Akiyama, K.; Shiono, M. & Negishi, N. (2003). DeBakey IIIb aortic dissection originating in a distal aortic arch aneurysm. *Ann. Thorac. Cardiovasc. Surg.,*Vol. 9(3):209-211.

Vorp, D.A.; Raghavan, M.L. & Webster, M.W. (1998). Mechanical Wall Stress in Abdominal Aortic Aneurysm: In°uence of Diameter and Asymmetry. *J. Vasc. Surg.,* Vol.27, pp.632-639.

Vorp, D.A.; Raghavan, M.L.; Muluk, S.C.; Makaroun, M.S.; Shapiro, R. & Webster, M.W. (1996). Wall Strength and Sti®ness of Aneurysmal and Nonaneurysmal Abdominal Aorta. *Ann. New York Acad. Sci.,* 800:274-277, 1996.

Xie, J.; Zhou, J. & Fung, Y.C. (1995). Bending of blood vessel wall: stress-strain laws of the intima-media and adventitial layers. J. Biomech. Eng., Vol. 117, pp. 136-145.

Qiao, A.; Liu, Y.; Chang, Y. & Matsuzawa, T. (2005). Computational study of stented aortic arch aneurysms. In: *27th Annual International Conference of the IEEE Engineering in Medicine and Biology Society*. Shanghai, China, September 2005.

Rhee, K.; Han, M.H. & Cha, S.H. (2002). Changes of flow characteristics by stenting in aneurysm models: influence of aneurysm geometry and stent porosity. *Ann. Biomed. Eng.* Vol.30, pp.894–904.

Ruiz, C.E.; Zhang, H.P.; Douglas, J.T.; Zuppan, C.W., & Kean, C.J. (1995). A novel method for treatment of abdominal aortic aneurysms using percutaneous implantation of a newly designed endovascular device. *Circulation* Vol.91, pp.2470–2477.
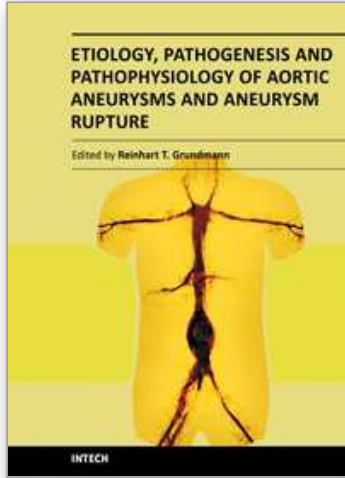
Etiology, Pathogenesis and Pathophysiology of Aortic Aneurysms and Aneurysm Rupture

Edited by Prof. Reinhart Grundmann

ISBN 978-953-307-523-5

Hard cover, 222 pages

Publisher InTech

Published online 27, July, 2011

Published in print edition July, 2011

This book considers mainly etiology, pathogenesis, and pathophysiology of aortic aneurysms (AA) and aneurysm rupture and addresses anyone engaged in treatment and prevention of AA. Multiple factors are implicated in AA pathogenesis, and are outlined here in detail by a team of specialist researchers. Initial pathological events in AA involve recruitment and infiltration of leukocytes into the aortic adventitia and media, which are associated with the production of inflammatory cytokines, chemokine, and reactive oxygen species. AA development is characterized by elastin fragmentation. As the aorta dilates due to loss of elastin and attenuation of the media, the arterial wall thickens as a result of remodeling. Collagen synthesis increases during the early stages of aneurysm formation, suggesting a repair process, but resulting in a less distensible vessel. Proteases identified in excess in AA and other aortic diseases include matrix metalloproteinases (MMPs), cathepsins, chymase and others. The elucidation of these issues will identify new targets for prophylactic and therapeutic intervention.

How to reference

In order to correctly reference this scholarly work, feel free to copy and paste the following:

Teruo Matsuzawa, Feng Gao, Aike Qiao, Osamu Ohta and Hiroshi Okada (2011). Numerical Simulation in Aortic Arch Aneurysm, Etiology, Pathogenesis and Pathophysiology of Aortic Aneurysms and Aneurysm Rupture, Prof. Reinhart Grundmann (Ed.), ISBN: 978-953-307-523-5, InTech, Available from: http://www.intechopen.com/books/etiology-pathogenesis-and-pathophysiology-of-aortic-aneurysms-and-aneurysm-rupture/numerical-simulation-in-aortic-arch-aneurysm

INTECH

open science | open minds